Journal of Environmental Management 323 (2022) 116193

Contents lists available at ScienceDirect

Journal of Environmental Management

journal homepage: www.elsevier.com/locate/jenvman

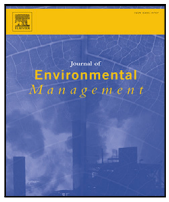

Research article

Heatwaves and fire in Pantanal: Historical and future perspectives from CORDEX-CORE

Patrícia S. Silva [a], João L. Geirinhas [a,*], Rémy Lapere [b], Wil Laura [c], Domingo Cassain [d], Andrés Alegría [e], Jayaka Campbell [f]

[a] Instituto Dom Luiz (IDL), Faculdade de Ciências, Universidade de Lisboa, Campo Grande, 1749-016, Lisboa, Portugal
[b] Laboratoire de Météorologie Dynamique, IPSL, École Polytechnique, Institut Polytechnique de Paris, CNRS, 91128 Palaiseau, France
[c] Servicio Nacional de Meteorología e Hidrología (SENAMHI), Lima, Peru
[d] Fundação Cearense de Meteorologia e Recursos Hídricos (FUNCEME), Ceará, Brazil
[e] Alfred Wegener Institute (AWI), Integrative Ecophysiology, Am Handelshafen 12, 27570 Bremerhaven, Germany
[f] Department of Physics, University of the West Indies, Mona Campus, Jamaica

ARTICLE INFO

Keywords:
Pantanal
Burned area
Heatwaves
CORDEX-CORE
RCP
Fire

ABSTRACT

The Pantanal biome, at the confluence of Brazil, Bolivia and Paraguay, is the largest continental wetland on the planet and an invaluable reserve of biodiversity. The exceptional 2020 fire season in Pantanal drew particular attention due to the severe wildfires and the catastrophic natural and socio-economic impacts witnessed within the biome. So far, little progress has been made in order to better understand the influence of climate extremes on fire occurrence in Pantanal. Here, we evaluate how extreme hot conditions, through heatwave events, are related to the occurrence and the exacerbation of fires in this region. A historical analysis using a statistical regression model found that heatwaves during the dry season explained 82% of the interannual variability of burned area during the fire season. In a future perspective, an ensemble of CORDEX-CORE simulations assuming different Representative Concentration Pathways (RCP2.6 and RCP8.5), reveal a significant increasing trend in heatwave occurrence over Pantanal. Compared to historical levels, the RCP2.6 scenario leads to more than a doubling in the Pantanal heatwave incidence during the dry season by the second half of the 21st century, followed by a plateauing. Alternatively, RCP8.5 projects a steady increase of heatwave incidence until the end of the century, pointing to a very severe scenario in which heatwave conditions would be observed nearly over all the Pantanal area and during practically all the days of the dry season. Accordingly, favorable conditions for fire spread and consequent large burned areas are expected to occur more often in the future, posing a dramatic short-term threat to the ecosystem if no preservation action is undertaken.

1. Introduction

The Pantanal biome is the largest continental wetland in the world, extending over parts of Brazil, Bergier and Assine (2016). This World Heritage Site (UNESCO, 2021) is home to a wide variety of plants (Pott et al., 2011) and animals (Alho, 2008), including several endangered species (Tomas et al., 2019). In 2020, Pantanal faced the most devastating fires in the last two decades. Satellite-derived estimates showed that around a third of the Brazilian section of Pantanal was affected (Libonati et al., 2020), including several indigenous territories and conservation units being completely burnt.

Fire activity and climate have been shown to be closely linked (Mariani et al., 2018; Abatzoglou et al., 2019; Ruffault et al., 2020; Sutanto et al., 2020) and the 2020 Pantanal fires resulted from an interplay between extreme hot and dry conditions (Libonati et al., 2022) associated with the negligent use of fire (Mataveli et al., 2020). Leading up to the 2020 fire season, Pantanal had been under severe drought conditions since 2019 (Marengo et al., 2021b), which severely impacted vegetation flammability. Soil desiccation conditions concurred with several heatwave episodes, leading to the establishment of strong soil moisture–temperature coupling regimes (water-limited) that triggered a temperature escalation through enhanced sensible heat fluxes from the surface to the atmosphere (Libonati et al., 2022). As a result of this, the compound dry and hot conditions observed during 2020 over Pantanal, essentially drove fire danger to levels not seen since 1980 (Libonati et al., 2020).

The future dynamics and intensity of global fires is uncertain under climate change scenarios, and highly depends on the climate zone and

* Corresponding author.
E-mail address: jlgeirinhas@fc.ul.pt (J.L. Geirinhas).

https://doi.org/10.1016/j.jenvman.2022.116193
Received 17 December 2021; Received in revised form 24 August 2022; Accepted 3 September 2022
Available online 20 September 2022

local human drivers (Moritz et al., 2012; Williams and Abatzoglou, 2016). For South America however, an increasing trend in fire risk and extent is projected under a range of likely scenarios (Cochrane and Barber, 2009; Liu et al., 2010; Silva et al., 2019; Burton et al., 2022; de Oliveira-Júnior et al., 2021; Oliveira et al., 2022). In parallel, the number of heatwaves associated with record-breaking temperatures have been increasing over Pantanal (Marengo et al., 2021b; Libonati et al., 2022). Such a growing trend in the number of extreme hot spells is expected to continue in most regions including South America (Dosio, 2017; Baker et al., 2018; Feron et al., 2019; Di Luca et al., 2020; Molina et al., 2020; Coppola et al., 2021). Feron et al. (2019) found for South America that the magnitude of this increase would not be spatially homogeneous, although by 2050, the tropical areas, including Pantanal, would witness extremely warm temperatures during at least half the days of the year. By the end of the century, annual average temperatures in Pantanal can increase by up to 7 °C relative to the 1961–1990 period (Marengo et al., 2015; Llopart et al., 2020). Additionally, daily maximum temperature in Pantanal will likely increase by several degrees over the period 2050–2080 under different scenarios (Reboita et al., 2021b). Although the effects of climate change on Pantanal remain by far uncertain and are probably outweighed by human development and wetland destruction (Junk, 2013), the possible trends can induce changes in the dynamics and properties of the fire season, possibly jeopardizing even more of Pantanal's ecosystems.

This work aims to evaluate the connection between heatwaves and fire in the Pantanal biome during the 2002–2020 period, and assess future trends under two climate change scenarios. Historical COordinated Regional Climate Downscaling EXperiment-COmmon Regional Experiment (CORDEX-CORE) simulations are then evaluated and compared to reanalysis data, evidencing the need for bias-correction. Accordingly, we compute bias-corrected future projections of heatwaves using the CORDEX-CORE ensemble and interpret the results in light of future climate change and what it might mean for fires in Pantanal.

2. Data and methods

2.1. Data

The region of interest is the Pantanal biome as defined by the Terrestrial Ecoregions of the World (Olson et al., 2001). Burned area was derived from the Moderate Resolution Imaging Spectroradiometer (MODIS) MCD64A1 Collection 6 product (Giglio et al., 2018), developed by the National Atmospheric Space Agency (NASA). Derived from the MODIS sensors aboard Terra and Aqua satellites, MCD64A1 is a monthly burned area product at a 500 m spatial resolution from 2001 to 2020. Re-projected GeoTIFF data for South America was obtained from the University of Maryland's fuoco SFTP Server (fuoco.geog.umd.edu). Burned area totals were computed for the Pantanal and 2001 was dropped as it only includes data from the MODIS sensor aboard Terra.

Daily maximum surface air temperature (Tmax) values from 1980 to present were obtained for Pantanal by computing the daily maximum of hourly surface temperatures retrieved from the European Centre of Medium-range Weather Forecast (ECMWF) ERA5 reanalysis dataset (Hersbach et al., 2020), at a gridded 0.25° × 0.25° spatial resolution.

Using data available from the ESGF platform (ESGF, 2014), simulated daily maximum temperature for the historical period (spanning 1981 to 2005) and Representative Concentration Pathways (RCP) 2.6 and 8.5 were extracted from CORDEX-CORE runs on the South American domain at a 0.22° spatial resolution (Gutowski et al., 2016; Giorgi et al., 2021). This work relies on three realizations (historical, RCP2.6 and RCP8.5) from two Regional Climate Models - RCMs (REMO2015, RegCM4-7), each one forced by three different Global Climate Models — GCMs (HadGEM2-ES, MPI-ESM, NorESM1) as described in Table 1. RCPs represent possible trajectories of future greenhouse gas and air pollutants emissions: the low-emission RCP2.6 scenario limits additional radiative forcing to 2.6 W/m^2 by 2100 (van Vuuren et al., 2011) whereas the high-emission RCP8.5 scenario corresponds to a 8.5 W/m^2 radiative forcing (Riahi et al., 2011).

Table 1
Regional climate models (RCM) considered in this study: runs for the South American domain at 0.22° × 0.22° spatial resolution (SAM-22) available within the COordinated Regional Climate Downscaling EXperiment-COmmon Regional Experiment (CORDEX-CORE; Giorgi et al. (2021)).

RCM	Experiment	Time period	Forced by
REMO2015	Historical	1981/01/01–2005/12/31	MOHC-HadGEM2-ES
	RCP2.6	2006/01/01–2099/12/31	MPI-M-MPI-ESM-LR
	RCP8.5	2006/01/01–2099/12/31	NCC-NorESM1-M
RegCM4-7	Historical	1981/01/01–2005/12/31	MOHC-HadGEM2-ES
	RCP2.6	2006/01/01–2099/12/31	MPI-M-MPI-ESM-MR
	RCP8.5	2006/01/01–2099/12/31	NCC-NorESM1-M

2.2. Heatwave definition

Using a relative threshold index (Perkins and Alexander, 2013; Geirinhas et al., 2021) heatwaves were defined as periods of three or more consecutive days featuring Tmax values above the climatological (1981–2010 in the case of data computation with ERA5, and 1981–2005 with the historical CORDEX-CORE simulations) calendar day 90th percentile (P90) of Tmax (centered on a 15-day window). Based on this definition, a single one dimensional variable accounting for the time and spatial incidence of heatwaves over Pantanal was defined: the percentage of the total Pantanal domain under heatwave conditions ($\%Pantanal_{HW}$). This metric was already used in previous studies conducted for regions within the USA (Mazdiyasni and AghaKouchak, 2015) and Brazil (Geirinhas et al., 2021), and consists in determining the percentage of the total Pantanal cells (in space and time - $cellsPAN_{total}$) that experience heatwave conditions ($cellsPAN_{HW}$), as expressed in Eq. (1).

$$\%Pantanal_{HW} = \frac{cellsPAN_{HW}}{cellsPAN_{total}} \times 100 \quad (1)$$

The number of total Pantanal cells ($cellsPAN_{total}$) is obtained by considering the total number of grid-points within the Pantanal region ($cellsPAN_{region}$) and the total number of days of the dry season (April through October - Fig. 1b - $cellsPAN_{time}$) as in Eq. (2).

$$cellsPAN_{total} = cellsPAN_{region} \times cellsPAN_{time} \quad (2)$$

The number of total Pantanal cells under heatwave ($cellsPAN_{HW}$) is computed in the exact same way as $cellsPAN_{total}$, however it only considers the number of days and grid-points that are under heatwave conditions (as defined earlier in this section). As an example of application, a percentage of 100% indicates that every single grid point in the Pantanal domain witnessed heatwave conditions for every day of the dry season, and so, $cellsPAN_{HW}$ equals $cellsPAN_{total}$.

2.3. Statistical analysis

The statistical relationship between burned area and heatwaves was evaluated using a simple linear regression model. Interannual variations of burned area (predictand, BA) were correlated with variations of the percentage of the total Pantanal domain under heatwave conditions (predictor, $\%Pantanal_{HW}$) as in Eq. (3).

$$BA = m \times \%Pantanal_{HW} + b \quad (3)$$

where m and b are the slope and intercept of the model, respectively. The goodness of fit was analyzed and assessed through the resulting coefficient of determination and p-value. To further test the robustness of the statistical model, and given the short length of the time series, a leave-one-out cross-validation scheme was performed (Wilks, 2011) and the Spearman's rank correlation coefficient computed.

Throughout this work, monotonic trends were estimated using the non-parametric Mann–Kendall two-tailed test (Mann, 1945; Kendall, 1975; Gilbert, 1987), and the Theil–Sen slope (Theil, 1950; Sen, 1968).

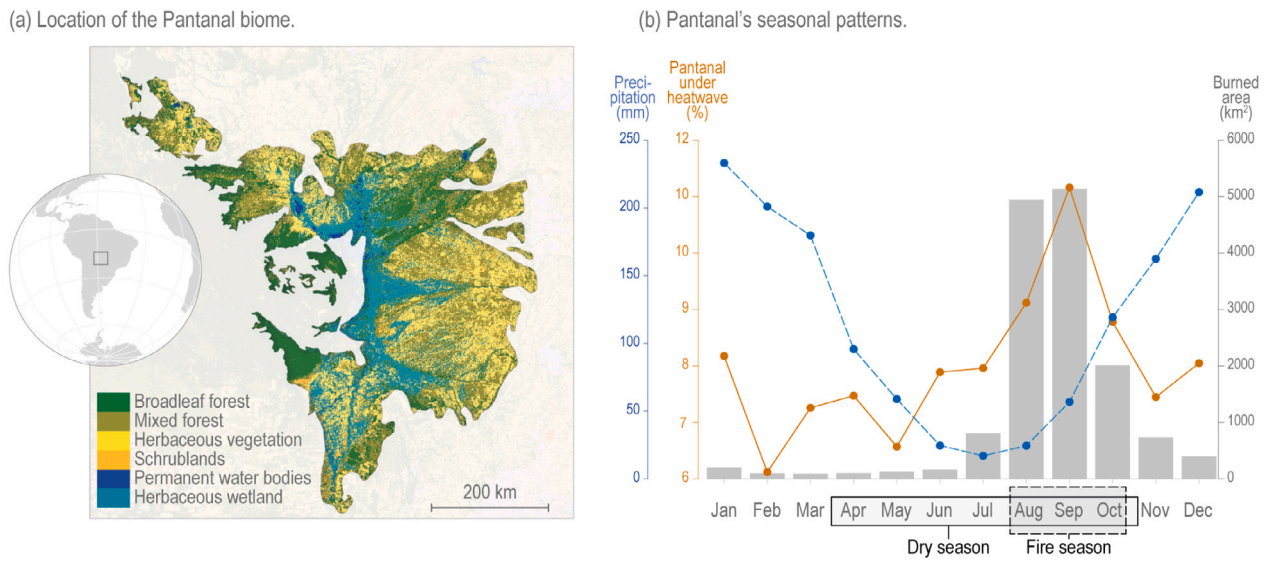

Fig. 1. (a) The Pantanal biome with land cover information for 2019 from the Copernicus Global Land Service (Buchhorn et al., 2020). (b) Pantanal's monthly averages of burned area (gray bars) as estimated by the MCD64A1 Collection 6 product over 2002–2020, and seasonal precipitation (blue line) and heatwave incidence (orange line) patterns in ERA5 reanalysis for the period 1981–2020. (For interpretation of the references to color in this figure legend, the reader is referred to the web version of this article.)

2.4. Bias correction

Bias correction was performed using a Quantile Delta Mapping (QDM) approach, in order to match Tmax distribution in the RCM realizations to that of ERA5, despite the discrepancies initially observed. The correction is applied both to historical and future scenario runs. QDM is known to perform well when it comes to preserving raw signals, trends and extremes (Cannon et al., 2015; Casanueva et al., 2020). QDM relies on the computation of the cumulative distribution functions (CDF) of the variable of interest, in the dataset of reference (here ERA5), and in the model to be adjusted on the historical and future periods (here CORDEX-CORE historical and RCPs). Based on these statistical distributions, the transformation applied can be summarized in Eq. (4). Using this approach, the bias corrected Tmax obtained with Eq. (4), referred to as $\mathrm{Tmax}_{FUT_{QDM}}$, will incorporate the climate change signals present in the original CORDEX-CORE RCP runs.

$$\mathrm{Tmax}_{FUT_{QDM}} = \mathrm{Tmax}_{FUT} \times \frac{CDF^{-1}_{ERA5}(CDF_{FUT}(\mathrm{Tmax}_{FUT}))}{CDF^{-1}_{HIST}(CDF_{FUT}(\mathrm{Tmax}_{FUT}))} \quad (4)$$

QDM can be performed either in a parametric or empirical approach to compute the CDF. Here, the choice of a parametric (thus continuous) rather than empirical (thus discrete) approach is made so as to be able to capture future extreme values that may not be reached in the historical period distribution. For well-chosen parametric distribution forms, the performance is similar for parametric and empirical approaches (Enayati et al., 2021). Further details on QDM and its suitability and performance for our purpose can be found in **Supplementary Material**, Figures S1 and S2.

3. Results

3.1. Fire-heatwave connection

Pantanal burns quite frequently and mostly during the period from August to October, henceforth referred to as the fire season (Fig. 1b; Damasceno-Junior et al. (2021)). These months account, on average, for 79% of the annual burned area over the study period and coincide with low rainfall levels. Heatwaves also occur more often and over larger areas during these three months, with the maximum value of $\%Pantanal_{HW}$ in September concurrent with the yearly peak in burned area. Heatwaves taking place in the austral summer (December, January, February) and during the transition from wet to dry season (March–April) are not associated with high burned areas as the vegetation is growing and moisture levels are high, which constrains the spread and extent of fires (Ivory et al., 2019). Accordingly, in the upcoming analysis we evaluate heatwave conditions over the months from April to October, considered here as the biome's dry season (Fig. 1b; Oliveira et al. (2014) and Ivory et al. (2019)), to account for the effects of heatwaves on fuel moisture levels prior to the fire season.

The biome averages 14,439 ± 9649 km^2 burned area (8.5 ± 5.7% of Pantanal's area) per year over the 2002–2020 time series, with high interannual variability (Fig. 2a). The years of 2002, 2019 and 2020, stand out as the most dramatic, with the latter burning a record-shattering amount unseen in Pantanal over the last two decades.

The interannual variability of burned area over the fire season seems to be closely related to the percentage of Pantanal that is under heatwave over the dry season (Fig. 2a). Years with the highest (lowest) burned area correspond with higher (lower) percentages of heatwave incidence over Pantanal ($\%Pantanal_{HW}$), with the exception of 2007, when the $\%Pantanal_{HW}$ reached its maximum value over the 2002–2019 period while burned area values were below the time series 75th percentile.

A simple linear regression model between annual values of these two variables obtained a Pearson coefficient of 0.90 (p-value < 0.001). Hence, the linear model described in Eq. (5) based on $\%Pantanal_{HW}$ significantly explains 82% of the variance of burned area over the 2002–2020 period (Fig. 2b). It is worth noting here that causality is not assumed in this relationship. It only constitutes a purely statistical conception that holds for values of $\%Pantanal_{HW}$ varying between approximately 3% to 34%, which is the historically observed range.

$$Burned\,Area = 0.88 \times \%Pantanal_{HW} - 0.97 \quad (5)$$

with burned area in 1000 km^2 and $\%Pantanal_{HW}$ in percentage.

The leave-one-out cross-validation scheme (**Supplementary Material**, Figure S3) resulted in a coefficient of determination of 0.78 between the observed and the predicted burned area values, and a Spearman's correlation ρ of 0.90 (p-value < 0.001), which confirms that the linear model is robust and indeed the best approach to correlate these variables.

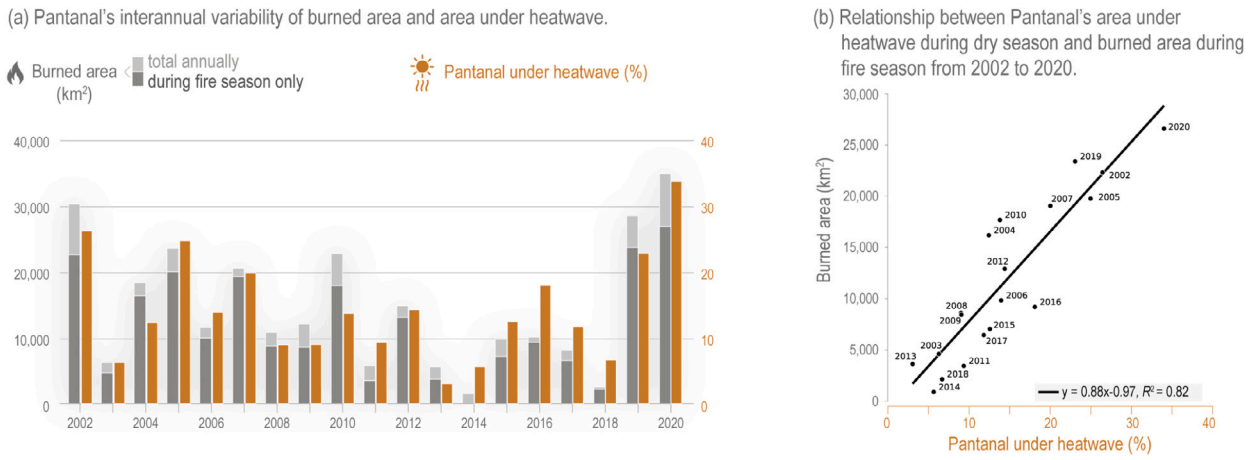

Fig. 2. (a) Interannual variability of annual burned area (light gray bars) and fire season burned area (August to October; dark gray bars), using the MODIS MCD64A1 product, and the percentage of Pantanal under heatwave ($\%Pantanal_{HW}$) over the dry season (April to October; orange bars), from 2002 to 2020. (b) Relationship between $\%Pantanal_{HW}$ over the dry season and the fire season burned area, estimated using ERA5 reanalysis, from 2002 to 2020, evaluated using simple linear regression model. Black line indicates the resulting regression line and on the bottom right corner is the corresponding equation. (For interpretation of the references to color in this figure legend, the reader is referred to the web version of this article.)

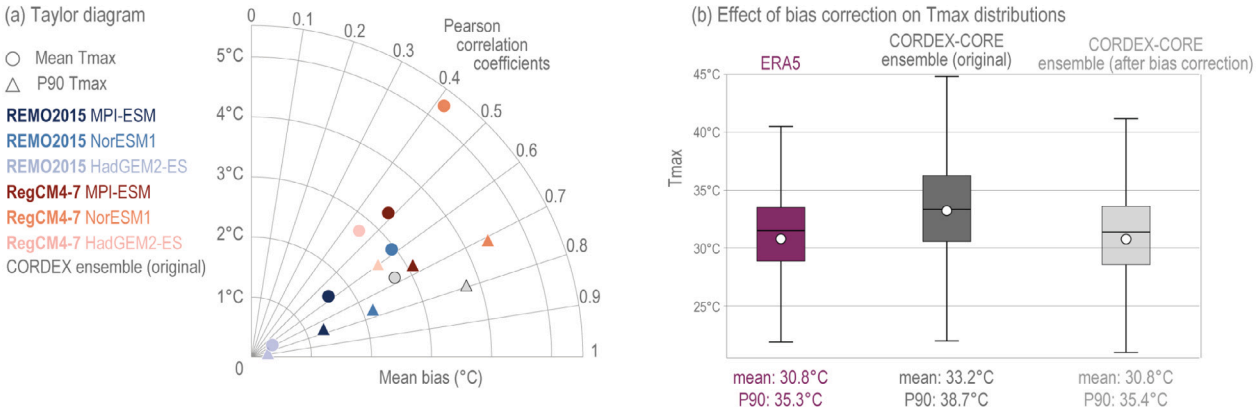

Fig. 3. (a) Taylor diagram of raw CORDEX-CORE historical simulations compared to ERA5. Tmax monthly mean (circles) and monthly P90 (triangles) during dry season months (April–October) over Pantanal for the period 1981–2005, for each simulation (color range) and for the ensemble mean (gray). All Pearson correlation coefficients presented here are statistically significant at the 99.9% level. (b) Tmax distribution over Pantanal for dry season months of the historical period in ERA5 (purple), CORDEX-CORE original (gray) and CORDEX-CORE after bias correction (light gray). (For interpretation of the references to color in this figure legend, the reader is referred to the web version of this article.)

3.2. Model evaluation

There is a large variability in the outcomes of each of the six members of the CORDEX-CORE ensemble considered. The comparison of Tmax between the six historical runs and the ERA5 reanalysis, for the Pantanal region, during the dry season and for the period 1981–2005, shows correlations on the time series of monthly averages of daily Tmax ranging from 0.42 to 0.67, and correlations on monthly P90 of Tmax between 0.60 and 0.84 (Fig. 3a). Mean biases on these variables are between 0.4 °C to 5.3 °C and 0.28 °C to 4.4 °C, for monthly averages and P90, respectively. REMO2015 forced by HadGEM2-ES shows the best agreement with ERA5, contrary to RegCM4-7 forced by NorESM1 that features the largest discrepancies with the ERA5 reanalysis. The remaining models show intermediate values and, for all models, lower mean biases and higher correlations are found when looking at the monthly P90. This large inter-model spread is commonly observed in multi-model analyses of RCMs, in particular in the CORDEX framework for South America (e.g. Feron et al., 2019). The ensemble is also shown to have a mean bias of 2.72 °C and 3.76 °C, and a Pearson correlation coefficient of 0.68 and 0.79, for the mean and P90 of Tmax, respectively. For impact studies, the ensemble mean is usually able to properly reproduce the main climatological features of the region, notwithstanding the large variability across individual members (Teichmann et al., 2021; Coppola et al., 2021).

Considering this inter-model variability and discrepancies compared to ERA5, Tmax datasets from the CORDEX-CORE runs were bias-corrected towards the distribution of Tmax in ERA5. Figure S1 shows the time series for Tmax of raw CORDEX-CORE historical data and both RCP runs over the 1981–2099 period, and the result after bias-correction. A clear shift is observed towards ERA5 values after bias correction, while keeping the trends intact. The performance of the bias correction is also illustrated in Fig. 3b, which shows that the bias between CORDEX-CORE and ERA5 ensemble mean (P90) Tmax goes from 2.4 °C (3.4 °C) before correction to less than 0.1 °C after. QDM therefore seems to be successful in approximating the CORDEX-CORE ensemble mean distribution to that of ERA5, as also evidenced in Figure S2. The bias-corrected results are now in the same range as those of the reanalysis: the historical mean of Tmax is now equal for CORDEX-CORE after QDM and the ERA5 reanalysis, at 30.8 °C (Fig. 3b). Moreover, Figure S1 confirms the above-mentioned large inter-model variability, with large shaded areas representing the maximum and minimum values simulated by CORDEX-CORE runs after bias-correction.

Figs. 4 and 5 further highlight this inter-model variability, which is found also in future projections. Under RCP8.5 scenario (Fig. 4), for the near future period (2026–2050, top line in the Figure), Tmax during the dry season increases on average between 0 to 2 °C approximately,

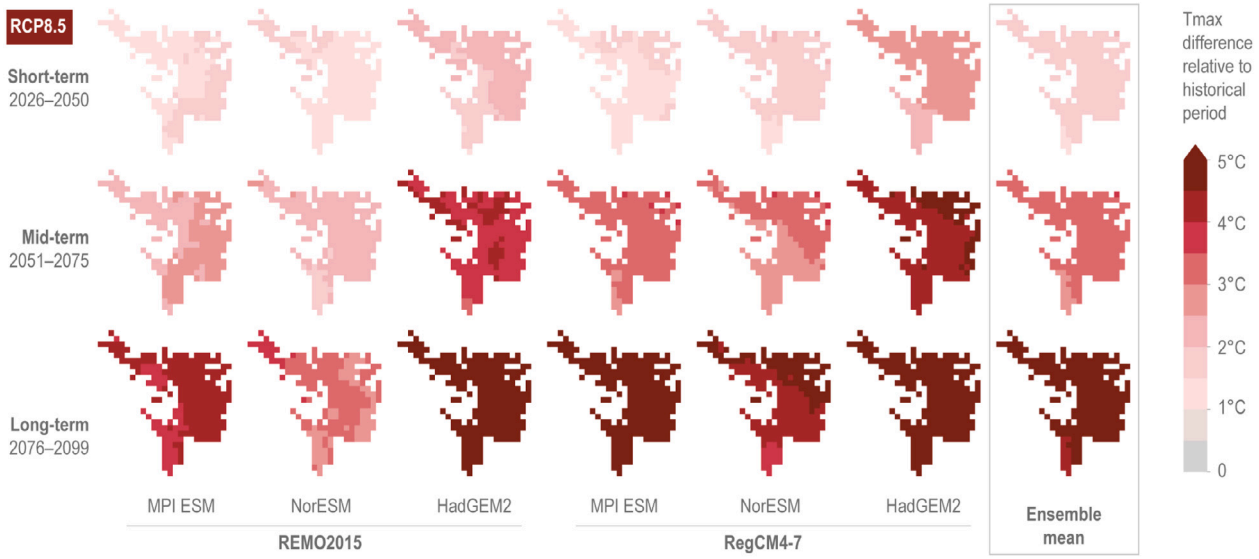

Fig. 4. Average difference on Tmax over the Pantanal region for April to October between the historical period and three projected RCP8.5 periods (2026–2050 as short term; 2051–2075 as mid term; and 2076–2099 as long term), for the six CORDEX-CORE simulations considered and the ensemble mean (rightmost panel). All data is from the bias-corrected simulations.

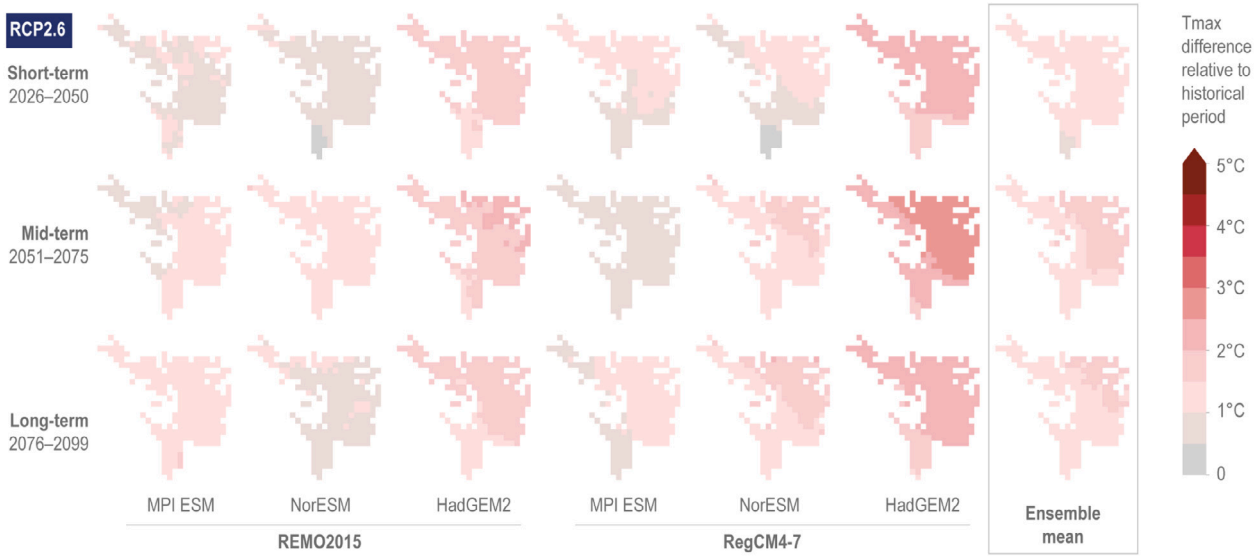

Fig. 5. Same as Fig. 4 for RCP2.6.

depending on the considered GCM/RCM combination. For the mid-term (2051–2075) and long-term (2076–2099) periods, the spread increases, with Tmax warming between 1.5 to 5 °C and 3 to 9 °C, respectively. The trajectory under RCP2.6 assumptions suggests a lesser warming of Pantanal, along with a smaller inter-model spread, in absolute value, as compared with RCP8.5 (Fig. 5). For that scenario, all runs feature an increase in Tmax between 0 to 4 °C without a clear temporal evolution, with Tmax departure from its historical values in the short-term being similar to the mid- and long-term periods ones. In both scenarios, the expected warming is spatially quite homogeneous over the Pantanal region, except for its southernmost part, which seems to be slightly less affected in most runs, as opposed to the northeastern part that might suffer from even warmer conditions by up to 1 °C according to several runs.

3.3. Future trends in heatwaves

We analyzed the simulated evolution of heatwaves over Pantanal from 1981 to the end of the 21st century, under scenarios RCP2.6 and RCP8.5, using CORDEX-CORE bias-corrected ensemble mean. Under both scenarios, the $\%Pantanal_{HW}$ is expected to increase by 2100 (Fig. 6), albeit with distinct growing patterns. Considering the optimistic emission scenario RCP2.6, the average $\%Pantanal_{HW}$ is expected to increase up to 36.4% over the mid-term period, followed by a decrease to 35.2% in the long-term period (Table 2). When compared to the historical average (12.5%), this represents a relative increase of 191% and 182% of the $\%Pantanal_{HW}$ for mid and long-term, respectively. Extremes, evaluated by the P90, reach 43.4% over mid-term and more than double the historical value with relative increases above 140% in all three time periods. However, no significant trend was found in either period, consistent with RCP2.6 assumptions of peaking emissions mid-century followed by a steady decrease afterwards (van Vuuren et al., 2011).

Alternatively, under the high-emission scenario RCP8.5 there is a statistically significant monotonic increase, clearly departing from the RCP2.6 scenario after the mid-term period, leading to a $\%Pantanal_{HW}$ level of 80% by the end of the 21st century (Fig. 6). Average (and P90)

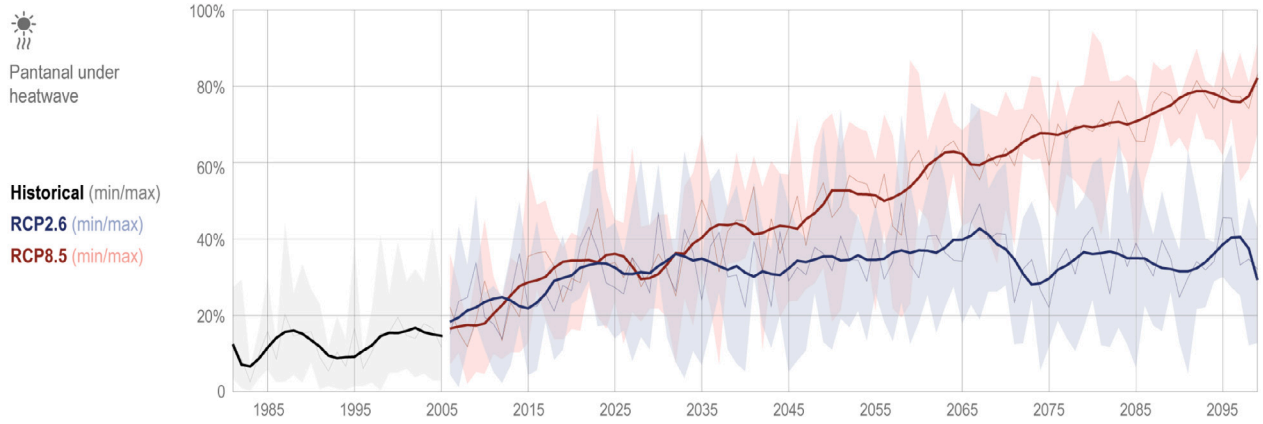

Fig. 6. Percentage of Pantanal under heatwave from 1981 to 2099. Evolution for historical (black line), RCP2.6 (blue line), and RCP8.5 (red line) bias-corrected CORDEX-CORE runs. The gray, blue and red shaded regions show the maximum range between individual model runs. Solid lines represent the ensemble mean and those that are thicker show a smoothed time series for better visualization. The smoothing is performed by applying a Savitzky–Golay filter with a window length of 19 years and a polynomial order 5. (For interpretation of the references to color in this figure legend, the reader is referred to the web version of this article.)

Table 2
Future evolution of heatwave index ($\%Pantanal_{HW}$) under RCP2.6 and RCP8.5 scenarios for three time periods: short-term from 2026 to 2050; mid-term from 2051 to 2075; and long-term from 2076 to 2099. For comparison, we further show values for the historical run from 1981 to 2005. Average values are calculated as ensemble mean from all RCM realizations. Std corresponds to the standard deviation, over time, of the ensemble mean for the considered period. Values between parentheses indicate relative change compared to the historical value. The presence of a trend is evaluated through the Mann–Kendall test at a 5% significance level. Upwards arrows indicate a significant positive trend. The average inter-model spread corresponds to the average, over each period, of the difference between the highest and lowest individual member values every year.

		Average	Std	P90	Trend	Inter-model spread
Historical		12.5	4.5	17.4	–	23.2
RCP2.6	Short-term	32.9 (163%)	6.6	41.8 (140%)	–	35.1
	Mid-term	36.4 (191%)	6.4	43.4 (149%)	–	32.8
	Long-term	35.2 (182%)	5.4	42.5 (144%)	–	33.9
RCP8.5	Short-term	39.9 (219%)	8.3	51 (193%)	↗	30.6
	Mid-term	58.5 (368%)	7.6	67.3 (287%)	↗	31.5
	Long-term	73.3 (486%)	4.6	78.4 (351%)	↗	24.1

values of $\%Pantanal_{HW}$ differ considerably over the three time periods (Table 2): from 39.9% (51%) in the short-term period, slightly above the corresponding values in RCP2.6, to 73.3% (78.4%) in the long-term period. In this scenario, departures from the mean (and P90) historical values are dramatic, with relative increases of 219% (193%), 368% (287%) and 486% (351%), for the short, mid and long-term periods, respectively.

Nevertheless, in both scenarios, inter-model variability is relatively large (Table 2). In particular, the spread of $\%Pantanal_{HW}$ between the minimum and maximum individual members from the ensemble for each projection year is around 32%, on average. In RCP2.6 scenario, this inter-model spread remains relatively stable, from 35% in the short-term period to 34% in the long-term, pointing to a moderate climate signal in Pantanal in that scenario. Contrarily, RCP8.5 leads to a decrease in the spread between models, from 31% in the short-term down to 24% in the last 25 years of the century. This indicates that under the stronger climate forcing of the RCP8.5 scenario, models tend to agree more on the long-term pathway as all of them foresee extreme heatwave conditions in Pantanal at the end of the century. For the RCP2.6 scenario, although the mean is clearly higher than historical values, the ensemble member with the lowest warming projection is indistinguishable from the historical envelope for all the time periods considered. On the other hand, the lowest warming projection for RCP8.5 is well above the maximum of the historical envelope despite a relatively large inter-model spread. In the first half of the century, individual simulations from both RCPs overlap (shaded areas in Fig. 6), however, after 2050 there is a clear distinction between the maximum and minimum simulated values obtained for each RCP (Fig. 6). By the end of the century, although the maximum simulated value of $\%Pantanal_{HW}$ under RCP2.6 is higher than that of the historical run, the historical simulations that achieved the highest $\%Pantanal_{HW}$ are in the same range of values as RCP2.6 $\%Pantanal_{HW}$ ensemble means. This is not the case with RCP8.5, where, by 2100, the minimum value of simulated $\%Pantanal_{HW}$ far exceeds the maximum value obtained in any historical simulation, highlighting how RCP8.5 is a much more severe scenario.

For both RCPs, inter-model variability seems to decrease over the 21st century, with model predictions converging towards the end of the simulation period. This is particularly sharp in RCP8.5 where there is a decrease in inter-model spread and standard deviations (Table 2), due to a threshold effect on the heatwave index computation, which is based on a comparison between Tmax and the fixed historical P90 of Tmax (see Section 2.2). In the case of RCP8.5 the significant increase in Tmax is such that, even though the inter-model variability in Tmax is large, all individual members are mostly above the historical heatwave threshold. Consequently, even the member with the lowest warming trajectory still generates a high heatwave index value, thereby dampening the variability observed in $\%Pantanal_{HW}$.

4. Discussion

The linear regression model developed in this study showed that 82% of the annual variance in Pantanal's burned area is related to annual variations in heatwave incidence. This strong connection between fire events and heatwaves is in agreement with previous analyses conducted worldwide (Chuvieco et al., 2021) and for Pantanal in particular (Viganó et al., 2018; Libonati et al., 2022). The occurrence of heatwaves over the dry season triggers large evaporation rates and thus soil desiccation that, ultimately, may influence the level of vegetation dryness and increase flammability. On the other hand, during the fire season heatwaves promote favorable conditions for larger burned areas if an ignition source is provided (which in the case of Pantanal is mostly human; Menezes et al. (2022)). Recent heatwave episodes in this region have been associated with the establishment of quasi-stationary anticyclonic circulation anomalies over central South America as a response of large-scale Rossby wave patterns forced by remote warm sea surface temperatures in Indian and Pacific oceans (e.g. ENSO, MJO, IOD) (Taschetto and Ambrizzi, 2012; Marengo et al., 2021a; Reboita et al., 2021a; Libonati et al., 2022). These mid-atmospheric

high pressure systems are responsible for strong subsidence and large amounts of incoming shortwave radiative energy at surface (Marengo et al., 2021a; Libonati et al., 2022; Geirinhas et al., 2022). On the other hand, they can induce large disturbances in the South Atlantic Convergence Zone (Nielsen et al., 2019) and/or in the South American Low-Level Jet (Montini et al., 2019) suppressing the passage of frontal systems and promoting the occurrence of large deficits in the water vapor transport from the Amazon basin towards Pantanal. A long-term shortage of moisture being advected from the Amazon basin coupled with a lower than normal atmospheric convergence in the region leverages large precipitation deficits and evaporation rates that, ultimately, promote a sharp decrease in soil moisture levels. In fact, Libonati et al. (2022) showed that during the 2020 fire season due to pronounced drought conditions over Pantanal, a strong soil moisture–temperature coupling (water-limited) was established allowing a re-amplification of the already established surface hot temperature anomalies during several heatwave episodes (Coronato et al., 2020; Geirinhas et al., 2022). As such, fire activity in Pantanal is also inevitably linked to drought and flood (Mataveli et al., 2020; Libonati et al., 2021; Marengo et al., 2021a). However, precipitation estimates show large inter-model discrepancies over South America (Solman et al., 2013; Falco et al., 2019; Solman and Blzquez, 2019) due to the commonly acknowledged shortcoming of RCMs when it comes to capturing precipitation. Accordingly, here the focus was made exclusively on the heatwave–fire connection.

Still, large biases were found in temperature estimates by the RCMs and, in order to legitimate the analysis of future heatwaves, the bias observed in CORDEX-CORE historical Tmax data with respect to ERA5 was corrected through QDM. Such an adjustment is required in order to obtain more plausible climate change projections, especially when it comes to extreme temperature-related phenomena (Iturbide et al., 2021). Although in this work the bias correction showed a good performance as evidenced in Table S1 and Figure S1, such approaches to adjust simulation data towards a better match with observations have known limitations and shortcomings. In particular, they can be considered statistical artifacts that do not provide clues on the credibility of the physical processes represented in the model (Maraun, 2016; Maraun et al., 2017). However, Maraun et al. (2017) recognize that for reasonably well captured physical processes, such as the ones driving the spatio-temporal variability of Tmax, usual bias correction methods work adequately. This is arguably the case here since the distribution of Tmax from ERA5 and from all the CORDEX-CORE models could be successfully fitted to the same class of theoretical distribution. These elements indicate that the underlying physical processes are consistently represented in the reanalysis and in the RCMs demonstrating that bias correction can be applied confidently. The choice of the bias correction technique is also known to condition the results obtained. Casanueva et al. (2020) and Iturbide et al. (2021) show that there are differences in the outputs of bias corrected models when different methods are applied to the same data, including Tmax in CMIP or CORDEX simulations, resulting in slightly different future projection scenarios. Nevertheless, the QDM applied here shows good performance to steer CORDEX-CORE data towards ERA5 values, and consistency in the climate signal between original and adjusted time series (Figure S1), which gives confidence in the conclusions of this study.

In particular, the climate change signal displaying increasing heatwave importance, and comparatively larger increase in RCP8.5 than in other scenarios, is consistent with previous studies investigating future trends in hot extremes. Despite differences in the projections, RCP4.5 and RCP8.5 scenarios are both known to lead to an increase in extreme temperature events, with larger changes over lower latitudes (Russo et al., 2014; Perkins-Kirkpatrick and Gibson, 2017; Feron et al., 2019). They also evidence, consistent with our findings, that heatwave future trends and levels are much worse under RCP8.5 scenario, across all of South America. Global warming will likely impose in Pantanal the occurrence of more intense and prolonged heatwaves due to linear increases of the mean surface temperature and non-linear feedbacks triggered by deep changes in precipitation, evaporation and radiative regimes (Donat et al., 2017; King, 2019). This raises new challenges not just for the ecosystems but also for human health and for other socio-economic sectors (e.g. agriculture and energy production). These threats are expected to be particularly relevant in low-income developing countries such as the ones that share the Pantanal biome (Brazil, Paraguay and Bolivia), where the public health services are fragile and where there is still a lack of investment in environmental protection policies. The heatwave projections highlighted here for Pantanal suggest that the heat-stress levels witnessed by the population of Pantanal will increase, leveraging the number of heat-related deaths to dramatic levels (Gasparrini et al., 2015; Guo et al., 2018).

Our results also suggest that such an increase in heatwave conditions could lead to higher burned areas, as favorable conditions for fire occurrence will occur more frequently and widespread over the region (Libonati et al., 2022). This could also trigger other cascading impacts of heatwaves in public health through the occurrence of more and widespread fires: a higher exposure to wildfire smoke is likely to lead to an increase in the number of respiratory illnesses and in birth defects not just for the living population of Pantanal but also for the inhabitants of downwind regions (Aguilera et al., 2021; Requia et al., 2021).

Nevertheless, such an increase in the heatwave index over the 21st century, and thus fire activity, would inevitably translate to changes in vegetation cover and climate–vegetation dynamics. Studies have found that fire influences the forest-savanna threshold (Hoffmann et al., 2012; Dantas et al., 2013) which means that such dramatic changes in fire activity could put several areas of Pantanal at risk of biome transition. As a result, these climate-fire-vegetation dynamics could change entirely the shape of the correlation between $\%Pantanal_{HW}$ and burned area for more intense heatwaves, which are not taken into account here as RCMs consider a static vegetation cover. For both scenarios, in addition, nonlinear vegetation-atmosphere and/or land–atmosphere feedback induced by climate change could also corrupt the climate assumptions on which our statistical regression model is based. Considering that the model assumes a climate stationarity, in that case the relation between heatwaves and fires would need to be adjusted and the model would need to be calibrated according to new climate conditions.

5. Conclusion

This study aimed at evaluating and modeling the connection between fire and heatwaves in Pantanal, and employed, for the first time, the CORDEX-CORE regional climate simulations at 0.22° spatial resolution, to project future heatwave estimates over the Pantanal biome. A robust connection was found between a heatwave index and burned area. A simple linear model based on $\%Pantanal_{HW}$ significantly explains 82% of the variance of burned area over the 2002–2020 period.

When looking at bias-corrected future projections of heatwaves by CORDEX-CORE model runs, we find that results differ considerably between scenarios, with RCP2.6, the low-emission scenario, reaching close to 40% of Pantanal under heatwave by mid-century to then stabilize to around 35% in 2100, whereas RCP8.5, the most severe scenario, shows a steady increase up to 80% by the end of the century.

The aforementioned ensemble means are associated with a large inter-model spread and therefore uncertainty. This spread is much smaller in RCP8.5 scenario indicating a stronger shift in heatwaves, with a significantly increasing trend. The lesser inter-model variability in heatwaves observed in the long-term in RCP8.5 compared to RCP2.6 reveals how extreme the former scenario is. In this trajectory, every model predicts maximum temperature occurrence and therefore heatwave frequency well above past values, thereby saturating the

historical thresholds. Possible changes in climate mechanisms and dynamics in the future (e.g. surface–atmosphere feedbacks) prevent the application of the statistical link between heatwaves and burned area that was evidenced in this study. However, this model can serve as a basis for educated guesses and qualitative assessments on possible future burned area, and suggests that under any scenario, even the more optimistic RCP2.6, burned area will likely increase, and the exceptional 2020 fire season in Pantanal could possibly compare as moderate with events in the near future.

Both fire (Alho et al., 2019) and climate change (Thielen et al., 2021) are major threats to the Pantanal biome, and the 2020 fire events were illustrative of the severe consequences it can have in biodiversity (Tomas et al., 2021), economy, and human health (Machado-Silva et al., 2020). The increased frequency of these fires is among the most visible results of human-induced climate change, posing a serious threat to biodiversity conservation, as the cumulative impact of widespread burning would be catastrophic if the situation of 2020 becomes common in the coming decades. Climate change may considerably alter the ecological properties of the Pantanal (Aparecido et al., 2021) which, associated with changes in land use and cover (Miranda et al., 2018; Colman et al., 2019; Marques et al., 2021), further contribute to a disturbed landscape and pave the way to increased fire activity (Kumar et al., 2022). Fire and land management are thus imperative within the Pantanal wetlands, to avoid further degradation to this unique ecosystem (Garcia et al., 2021; Berlinck et al., 2022).

As to the authors' knowledge this is the first study evaluating fire and heatwaves over the Pantanal biome, employing a set of regional climate simulations of relatively-high spatial resolution to project future trends. Very little research has been done in climate extremes over this region and more so is needed to properly understand the physical mechanisms associated with the found heatwave–fire relationship. These results provide useful information for fire activity in the biome in light of future climate change, and may also assist with regional information of the connection between fire and heatwaves in Pantanal to improve statistical or physical models.

CRediT authorship contribution statement

Patrícia S. Silva: Conceptualization, Methodology, Formal analysis, Writing – original draft, Visualization, Supervision. **João L. Geirinhas:** Conceptualization, Methodology, Formal analysis, Writing – original draft. **Rémy Lapere:** Conceptualization, Formal analysis, Data curation, Writing – original draft, Visualization. **Wil Laura:** Formal analysis, Data curation, Writing – original draft, Visualization. **Domingo Cassain:** Data curation, Writing – original draft. **Andrés Alegría:** Data visualization. **Jayaka Campbell:** Writing – original draft.

Declaration of competing interest

The authors declare that they have no known competing financial interests or personal relationships that could have appeared to influence the work reported in this paper.

Data availability

Data will be made available on request

Acknowledgments

This collaborative research is the product of a capacity building activity organized by CORDEX-WCRP to promote collaborative activities and networking and to enhance the capacity to document scientific research in Central America and the Caribbean, and South America with focus on specific regional climate phenomena (http://www.cima.fcen.uba.ar/cordex-2020/). P.S.S. and J.L.G. were supported by the Portuguese Fundação para a Ciência e a Tecnologia (FCT), Portugal [grants SFRH/BD/146646/2019 and 2020.05198.BD], and this work was funded by the Portuguese Fundação para a Ciência e a Tecnologia (FCT) I.P./MCTES through national funds (PIDDAC) – UIDB/50019/2020. The authors also acknowledge Maria Laura Bettolli, Renata Libonati and Carlos C. DaCamara, for their constructive comments on this work.

Appendix A. Supplementary data

Supplementary material related to this article can be found online at https://doi.org/10.1016/j.jenvman.2022.116193. This document provides further information on the bias correction method and robustness of the statistical relationship between burned area and heatwaves.

References

Abatzoglou, J., Williams, A., Barbero, R., 2019. Global emergence of anthropogenic climate change in fire weather indices. Geophys. Res. Lett. 46, 326–336. http://dx.doi.org/10.1029/2018GL080959.

Aguilera, R., Corringham, T., G, A., et al., 2021. Wildfire smoke impacts respiratory health more than fine particles from other sources: observational evidence from southern california. Nature Commun. 12, 1493. http://dx.doi.org/10.1038/s41467-021-21708-0.

Alho, C., 2008. Biodiversity of the pantanal: response to seasonal flooding regime and to environmental degradation. Braz. J. Biol. 68, http://dx.doi.org/10.1590/S1519-69842008000500005.

Alho, C.R., Mamede, S.B., Benites, M., Andrade, B.S., Sepú, J.J.O., 2019. Threats to the biodiversity of the Brazilian pantanal due to land use and occupation. Ambient. Soc. 22, 22:e01891. http://dx.doi.org/10.1590/1809-4422asoc201701891vu2019L3AO.

Aparecido, L., Lorençone, P., Lorençone, J., Meneses, K., Moraes, J.S., 2021. Climate changes and their influences in water balance of pantanal biome. Theor. Appl. Climatol. 143, 659–674. http://dx.doi.org/10.1007/s00704-020-03445-4.

Baker, H.S., Millar, R.J., Karoly, D.J., Beyerle, U., Guillod, B.P., Mitchell, D., Shiogama, H., Sparrow, S., Woollings, T., Allen, M.R., 2018. Higher CO_2 concentrations increase extreme event risk in a 1.5 °C world. Nature Clim. Change 8, 604–608. http://dx.doi.org/10.1038/s41558-018-0190-1.

Bergier, I., Assine, M.L., 2016. Dynamics of the Pantanal Wetland in South America. Springer, http://dx.doi.org/10.1007/978-3-319-18735-8.

Berlinck, C.N., Lima, L.H.A., Pereira, A.M.M., Jr., E.A.R.C., Paula, R.C., Thomas, W.M., Morato, R.G., 2022. The pantanal is on fire and only a sustainable agenda can save the largest wetland in the world. Braz. J. Biol. 82, e244200. http://dx.doi.org/10.1590/1519-6984.244200.

Buchhorn, M., Smets, B., Bertels, L., De Roo, B., Lesiv, M., Tsendbazar, N.-E., Herold, M., Fritz, S., 2020. Copernicus Global Land Service: Land Cover 100 M: Collection 3: Epoch 2015: Globe. Zenodo, http://dx.doi.org/10.5281/zenodo.3518038.

Burton, C., Kelley, D.I., Jones, C.D., Betts, R.A., Cardoso, M., Anderson, L., 2022. South American fires and their impacts on ecosystems increase with continued emissions. Climate Resilience and Sustainability 1, e8. http://dx.doi.org/10.1002/cli2.8.

Cannon, A., Sobie, S., Murdock, T., 2015. Bias correction of GCM precipitation by quantile mapping: how well do methods preserve changes in quantiles and extremes? 28, 6938–6959. http://dx.doi.org/10.1175/JCLI-D-14-00754.1.

Casanueva, A., Herrera, S., Iturbide, M., Lange, S., Jury, M., Dosio, A., Maraun, D., Gutiérez, J., 2020. Testing bias adjustment methods for regional climate change applications under observational uncertainty and resolution mismatch. Atmos. Sci. Lett. 21, 978. http://dx.doi.org/10.1002/asl.978.

Chuvieco, E., Pettinari, M., Koutsias, N., Forkel, M., Hantson, S., Turco, M., 2021. Human and climate drivers of global biomass burning variability. Sci. Total Environ. 779, 146361. http://dx.doi.org/10.1016/j.scitotenv.2021.146361.

Cochrane, M., Barber, C., 2009. Climate change, human land use and future fires in the amazon. Glob. Change Biol. 15, 601–612. http://dx.doi.org/10.1111/j.1365-2486.2008.01786.x.

Colman, C.B., Oliveira, P.T.S., Almagro, A., Soares-Filho, B.S., Rodrigues, D.B.B., 2019. Effects of climate and land-cover changes on soil erosion in Brazilian pantanal. Sustainability 11, 7053. http://dx.doi.org/10.3390/su11247053.

Coppola, E., Raffaele, F., Giorgi, F., 2021. Climate hazard indices projections based on CORDEX-CORE, CMIP5 and CMIP6 ensemble. Clim. Dyn. http://dx.doi.org/10.1007/s00382-021-05640-z.

Coronato, T., Carril, A.F., Zaninelli, P., et al., 2020. The impact of soil moisture–atmosphere coupling on daily maximum surface temperatures in southeastern south America. Clim. Dyn. 55, 2543–2556. http://dx.doi.org/10.1007/s00382-020-05399-9.

Damasceno-Junior, G., de Roque, F., Garcia, L., Bandini Ribeiro, D., Scremin-Dias, E., Dias, F., Libonati, R., Rodrigues, J., Lemos, F., e. a. Santos, M., 2021. Lessons to be learned from the wildfire catastrophe of 2020 in the pantanal wetland. Wetl. Sci. Pract. 38, 107–115.

Dantas, V.L., Batalha, M.A., Pausas, J.G., 2013. Fire drives functional thresholds on the savanna–forest transition. Ecology 94, 2454–2463. http://dx.doi.org/10.1890/12-1629.1.

de Oliveira-Júnior, J.F., Mendes, D., Filho, W.L.F.C., da Silva Junior, C.A., de Gois, G., da Rosa Ferraz Jardim, A.M., da Silva, M.V., Lyra, G.B., Teodoro, P.E., Pimentel, L.C.G., Lima, M., de Barros Santiago, D., Rogério, J.P., Marinho, A.A.R., 2021. Fire foci in south America: Impact and causes, fire hazard and future scenarios. J. South Am. Earth Sci. 112, 103623. http://dx.doi.org/10.1016/j.jsames.2021.103623.

Di Luca, A., de Elía, R., Bador, M., Argüeso, D., 2020. Contribution of mean climate to hot temperature extremes for present and future climates. Weather Clim. Extrem. 28, 100255. http://dx.doi.org/10.1016/j.wace.2020.100255.

Donat, M.G., Pitman, A.J., Seneviratne, S.I., 2017. Regional warming of hot extremes accelerated by surface energy fluxes. Geophys. Res. Lett. 44, 7011–7019. http://dx.doi.org/10.1002/2017GL073733.

Dosio, A., 2017. Projection of temperature and heat waves for Africa with an ensemble of CORDEX regional climate models. Clim. Dyn. 49, 493–519. http://dx.doi.org/10.1007/s00382-016-3355-5.

Enayati, M., Bozorg-Hadda, O., Bazrafshan, J., Hejabi, S., Chu, X., 2021. Bias correction capabilities of quantile mapping methods for rainfall and temperature variables. J. Water Clim. Change 12, 401–419. http://dx.doi.org/10.2166/wcc.2020.261.

ESGF, 2014. The earth system grid federation: An open infrastructure for access to distributed geospatial data. Future Gener. Comput. Syst. 36, 400–417. http://dx.doi.org/10.1016/j.future.2013.07.002.

Falco, M., Carril, A., Menéndez, C., Zaninelli, P., Li, L., 2019. Assessment of CORDEX simulations over south America: added value on seasonal climatology and resolution considerations. Clim. Dyn. 52, 4771–4786. http://dx.doi.org/10.1007/s00382-018-4412-z.

Feron, S., Cordero, R., Damiani, A., Llanillo, P., Jorquera, J., Sepulveda, E., Asencio, V., Laroze, D., Labbe, F., Carrasco, J., Torres, G., 2019. Observations and projections of heat waves in south America. Sci. Rep. 9, 8173. http://dx.doi.org/10.1038/s41598-019-44614-4.

Garcia, L.C., Szabo, J.K., de Oliveira Roque, F., Pereira, A.M.M., da Cunha, C., Damasceno-Junior, G.A., Morato, R.G., Tomas, W.M., Libonati, R., Ribeiro, D.B., 2021. Record-breaking wildfires in the world's largest continuous tropical wetland: Integrative fire management is urgently needed for both biodiversity and humans. J. Environ. Manag. 293, 112870. http://dx.doi.org/10.1016/j.jenvman.2021.112870.

Gasparrini, A., Guo, Y., H, M., et al., 2015. Mortality risk attributable to high and low ambient temperature: a multicountry observational study. Lancet 386, 369–375. http://dx.doi.org/10.1016/S0140-6736(14)62114-0.

Geirinhas, J.L., Russo, A.C., Libonati, R., Miralles, D.G., Sousa, P.M., Wouters, H., Trigo, R.M., 2022. The influence of soil dry-out on the record-breaking hot 2013/2014 summer in southeast Brazil. Sci. Rep. 12, 5836. http://dx.doi.org/10.1038/s41598-022-09515-z.

Geirinhas, J.L., Russo, A., Libonati, R., Sousa, P., Miralles, D., Trigo, R., 2021. Recent increasing frequency of compound summer drought and heatwaves in southeast Brazil. Envion. Res. Lett. 16, 034036. http://dx.doi.org/10.1088/1748-9326/abe0eb.

Giglio, L., Boschetti, L., Roy, D., Humber, M., Justice, C., 2018. The collection 6 MODIS burned area mapping algorithm and product. http://dx.doi.org/10.1016/j.rse.2018.08.005.

Gilbert, R., 1987. Sen's nonparametric estimator of slope. In: Statistical Methods for Environmental Pollution Monitoring. John Wiley & Sons, pp. 217–219.

Giorgi, F., Coppola, E., Jacob, D., Teichmann, C., Omar, S.A., Ashfaq, M., Ban, N., Bülow, K., Bukovsky, M., Buntemeyer, L., Cavazos, T., Ciarló, J., Rocha, R.P.D., Das, S., di Sante, F., Evans, J.P., Gao, X., Giuliani, G., Glazer, R.H., Hoffmann, P., Im, E.-S., Langendijk, G., Lierhammer, L., Llopart, M., Mueller, S., Luna-Nino, R., Nogherotto, R., Pichelli, E., Raffaele, F., Reboita, M., Rechid, D., Remedio, A., Remke, T., Sawadogo, W., Sieck, K., Torres-Alavez, J.A., Weber, T., 2021. The CORDEX-CORE EXP-i initiative: Description and highlight results from the initial analysis. Bull. Am. Meteorol. Soc. 1–52. http://dx.doi.org/10.1175/BAMS-D-21-0119.1.

Guo, Y., Gasparrini, A., Li, S., Sera, F., Vicedo-Cabrera, A.M., de Sousa, Z.S.C.M., et al., 2018. Quantifying excess deaths related to heatwaves under climate change scenarios: A multicountry time series modelling study. PLoS Med. 15, e1002629. http://dx.doi.org/10.1371/journal.pmed.1002629.

Gutowski, W.J., Giorgi, F., Timbal, B., Frigon, A., Jacob, D., Kang, H.-S., Raghavan, K., Lee, B., Lennard, C., Nikulin, G., O'Rourke, E., Rixen, M., Solman, S., Stephenson, T., Tangang, F., 2016. WCRP coordinated regional downscaling experiment (CORDEX): a diagnostic MIP for CMIP6. Geosci. Model Dev. 9, 4087–4095. http://dx.doi.org/10.5194/gmd-9-4087-2016.

Hersbach, H., Bell, B., Berrisford, P., 2020. The ERA5 global reanalysis. Q. J. R. Meteorol. Soc. 146, 1999–2049. http://dx.doi.org/10.1002/qj.3803.

Hoffmann, W.A., Geiger, E.L., Gotsch, S.G., Rossatto, D.R., Silva, L.C.R., Lau, O.L., Haridasan, M., Franco, A.C., 2012. Ecological thresholds at the savanna-forest boundary: how plant traits, resources and fire govern the distribution of tropical biomes. Ecol. Lett. 15, 759–768. http://dx.doi.org/10.1111/j.1461-0248.2012.01789.x.

Iturbide, M., Casanueva, A., Bedia, J., Herrera, S., Milovac, J., Gutiérrez, J.M., 2021. On the need of bias adjustment for more plausible climate change projections of extreme heat. Atmos. Sci. Lett. 23, e1072. http://dx.doi.org/10.1002/asl.1072.

Ivory, S., McGlue, M., Spera, S., Silva, A., Bergier, I., 2019. Vegetation, rainfall, and pulsing hydrology in the pantanal, the world's largest tropical wetland. Environ. Res. Lett. 14, 124017. http://dx.doi.org/10.1088/1748-9326/ab4ffe.

Junk, W., 2013. Current state of knowledge regarding south america wetlands and their future under global climate change. Aquat. Sci. 75, 113–131. http://dx.doi.org/10.1007/s00027-012-0253-8.

Kendall, M., 1975. Rank Correlation Methods. Griffin, London.

King, A.D., 2019. The drivers of nonlinear local temperature change under global warming. Environ. Res. Lett. 14, 064005. http://dx.doi.org/10.1088/1748-9326/ab1976.

Kumar, S., Getirana, A., Libonati, R., Hain, C., Mahanama, S., Andela, N., 2022. Changes in land use enhance the sensitivity of tropical ecosystems to fire-climate extremes. Sci. Rep. 12, 964. http://dx.doi.org/10.1038/s41598-022-05130-0.

Libonati, R., DaCamara, C., Peres, L., Carvalho, L., Garcia, L., 2020. Rescue Brazil's burning pantanal wetlands. Nature 588, 217–219. http://dx.doi.org/10.1038/d41586-020-03464-1.

Libonati, R., Geirinhas, J.L., Silva, P.S., Russo, A., Rodrigues, J.A., Belém, L.B.C., Nogueira, J., Roque, F.O., DaCamara, C.C., Nunes, A.M.B., Marengo, J.A., Trigo, R.M., 2022. Assessing the role of compound drought and heatwave events on unprecedented 2020 wildfires in the pantanal. Environ. Res. Lett. 17, 015005. http://dx.doi.org/10.1088/1748-9326/ac462e.

Libonati, R., Pereira, J., Da Camara, C.e.a., 2021. Twenty-first century droughts have not increasingly exacerbated fire season severity in the Brazilian amazon. Sci. Rep. 11, 4400. http://dx.doi.org/10.1038/s41598-021-82158-8.

Liu, Y., Stanturf, J., Goodrick, S., 2010. Trends in global wildfire potential in a changing climate. For. Ecol. Manag. 259, 685–697. http://dx.doi.org/10.1016/j.foreco.2009.09.002.

Llopart, M., Simões Reboita, M., Rocha, R., 2020. Assessment of multi-model climate projections of water resources over south America CORDEX domain. Clim. Dyn. 54, 99–116. http://dx.doi.org/10.1007/s00382-019-04990-z.

Machado-Silva, F., Libonati, R., de Lima, T.F.M., Peixoto, R.B., de Almeida Fran ç, J.R., de Avelar Figueiredo Mafra Magalhã, M., Santos, F.L.M., Rodrigues, J.A., DaCamara, C.C., 2020. Drought and fires influence the respiratory diseases hospitalizations in the amazon. Ecol. Indic. 109, 105817. http://dx.doi.org/10.1016/j.ecolind.2019.105817.

Mann, H., 1945. Nonparametric tests against trend. Econometrica 245–259. http://dx.doi.org/10.2307/1907187.

Maraun, D., 2016. Bias correcting climate change simulations – a critical review. Curr. Clim. Change Rep. 2, 211–220. http://dx.doi.org/10.1007/s40641-016-0050-x.

Maraun, D., Shepherd, T., Widmann, M., 2017. Towards process-informed bias correction of climate change simulations. Nature Clim. Change 7, 764–773. http://dx.doi.org/10.1038/nclimate3418.

Marengo, J., Ambrizzi, T., Barreto, N., Cunha, A., Ramos, A., Skansi, M., Carpio, J., Salinas, R., 2021a. The heat wave of 2020 in central south America. Int. J. Climatol. 1, 18. http://dx.doi.org/10.1002/joc.7365.

Marengo, J., Cunha, A., Cuartas, L., Leal, K., Broedel, E., Seluchi, M., Michelin, C., Baião, C., ngulo, E., Almeida, E., Kazmierczak, M., Mateus, N., Silva, R., Bender, F., 2021b. Extreme drought in the Brazilian pantanal in 2019–2020: Characterization, causes, and impacts, front. Water 3, 639204. http://dx.doi.org/10.3389/frwa.2021.639204.

Marengo, J., Oliveira, G., Alves, L., 2015. Climate change scenarios in the pantanal. In: Bergier, A.M.I. (Ed.), Dynamics of the Pantanal Wetland in South America, Vol. 37. Springer, pp. 227–238. http://dx.doi.org/10.1007/698-2015-357.

Mariani, M., Holz, A., Veblen, T., Williamson, G., Fletcher, M., Bowman, D., 2018. Climate change amplifications of climate–fire teleconnections in the southern hemisphere. Geophys. Res. Lett. 45, 5071–5081. http://dx.doi.org/10.1029/2018GL078294.

Marques, J.F., Alves, M.B., Silveira, C.F., Silva, A.A., Silva, T.A., Santos, V.J., Calijuri, M.L., 2021. Fires dynamics in the pantanal: Impacts of anthropogenic activities and climate change. J. Environ. Manag. 299, 113586. http://dx.doi.org/10.1016/j.jenvman.2021.113586.

Mataveli, G., Pereira, G., Oliveira, G., Seixas, H., Cardozo, F., Shimabukuro, Y., Kawakubo, F., Brunsell, N., 2020. Pantanal's widespread fire: short- and long-term implications for biodiversity and conservation. Biodivers. Conserv. 2021. http://dx.doi.org/10.1007/s10531-021-02243-2.

Mazdiyasni, O., AghaKouchak, A., 2015. Substantial increase in concurrent droughts and heatwaves in the United States. Proc. Natl. Acad. Sci. USA 112, 11484–11489. http://dx.doi.org/10.1073/pnas.1422945112.

Menezes, L.S., Oliveira, A.M., Santos, F.L.M., Russo, A., de Souza, R.A.F., Roque, O.F., Libonati, R., 2022. Lightning patterns in the pantanal: Untangling natural and anthropogenic-induced wildfires. Sci. Tot. Environ. 820, 153021. http://dx.doi.org/10.1016/j.scitotenv.2022.153021.

Miranda, C.S., Filho, A.C.P., Pott, A., 2018. Changes in vegetation cover of the pantanal wetland detected by vegetation index: a strategy for conservation. Biota Neotrop. 18, e20160297. http://dx.doi.org/10.1590/1676-0611-BN-2016-0297.

Molina, M., Snchez, E., Gutiérez, C., 2020. Future heat waves over the mediterranean from an euro-CORDEX regional climate model ensemble. Sci. Rep. 10, 8801. http://dx.doi.org/10.1038/s41598-020-65663-0.

Montini, T.L., Jones, C., Carvalho, L.M.V., 2019. The south American low-level jet: A new climatology. J. Geophys. Res. 124, 1200–1218. http://dx.doi.org/10.1029/2018JD029634.

Moritz, M., Parisien, M.-A., Batllori, E., Krawchuk, M., Van Dorn, J., Ganz, D., Hayhoe, K., 2012. Climate change and disruptions to global fire activity. Ecosphere 3, 49. http://dx.doi.org/10.1890/ES11-00345.1.

Nielsen, D.M., Belém, A.L., Marton, E., Cataldi, M., 2019. Dynamics-based regression models for the south Atlantic convergence zone. Clim. Dyn. 52, 5527–5553. http://dx.doi.org/10.1007/s00382-018-4460-4.

Oliveira, M.T., Damasceno-Juniora, G.A., Pott, A., Filho, A.C.P., Suarez, Y.R., Parolin, P., 2014. Regeneration of riparian forests of the Brazilian pantanal under flood and fire influence. For. Ecol. Manag. 331, 256–263. http://dx.doi.org/10.1016/j.foreco.2014.08.011.

Oliveira, U., Soares-Filho, B., Bustamante, M., Gomes, L., Ometto, J.P., Rajao, R., 2022. Determinants of fire impact in the Brazilian biomes. Front. Glob. Change 5, 735017. http://dx.doi.org/10.3389/ffgc.2022.735017.

Olson, D., Dinerstein, E., Wikramanayake, E., Burgess, N., Powell, G., Underwood, E., D'amico, J., Itoua, I., Strand, H., Morrison, J., Loucks, C., Allnutt, T., Ricketts, T., Kura, Y., Lamoreux, J., Wettengel, W., Hedao, P., Kassem, K., 2001. Terrestrial ecoregions of the world: A new map of life on earth: A new global map of terrestrial ecoregions provides an innovative tool for conserving biodiversity. BioScience 51, 933–938. http://dx.doi.org/10.1641/0006-3568(2001)051.

Perkins, S., Alexander, L., 2013. On the measurement of heat waves. 26, 4500–4517. http://dx.doi.org/10.1175/JCLI-D-12-00383.1.

Perkins-Kirkpatrick, S.E., Gibson, P.B., 2017. Changes in regional heatwave characteristics as a function of increasing global temperature. Sci. Rep. 7, 12256. http://dx.doi.org/10.1038/s41598-017-12520-2.

Pott, A., Oliveira, A., Damasceno-Junior, G., Silva, J., 2011. Plant diversity of the pantanal wetland. Braz. J. Biol. 71, http://dx.doi.org/10.1590/S1519-69842011000200005.

Reboita, M.S., Ambrizzi, T., Crespo, N.M., Dutra, L.M.M., Ferreira, G.W. de S., Rehbein, A., Drumond, A., da Rocha, R.P., de Souza, C.A., 2021a. Impacts of teleconnection patterns on south America climate. Ann. New York Acad. Sci. 1504, 116–153. http://dx.doi.org/10.1111/nyas.14592.

Reboita, M., Kuki, C., Marrafon, V., et al., 2021b. South America climate change revealed through climate indices projected by GCMs and eta-RCM ensembles. Clim. Dyn. http://dx.doi.org/10.1007/s00382-021-05918-2.

Requia, W.J., Kill, E., P, S., et al., 2021. Prenatal exposure to wildfire-related air pollution and birth defects in Brazil. J. Expo. Sci. Environ. http://dx.doi.org/10.1038/s41370-021-00380-y.

Riahi, K., Rao, S., Krey, V., Cho, C., Chirkov, V., Fischer, G., Kindermann, G., Nakicenovic, N., Rafaj, P., 2011. RCP8.5 - a scenario of comparatively high greenhouse gas emissions. Clim. Change 109, 33. http://dx.doi.org/10.1007/s10584-011-0149-y.

Ruffault, J., Curt, T., Moron, V., Trigo, R., Mouillot, F., Koutsias, N., Pimont, F., Martin-StPaul, N., Barbero, R., Dupuy, J.-L., Russo, A., Belhadj-Khedher, C., 2020. Increased likelihood of heat-induced large wildfires in the mediterranean basin. Sci. Rep. 10, 13790. http://dx.doi.org/10.1038/s41598-020-70069-z.

Russo, S., Dosio, A., Graversen, R.G., Sillmann, J., Carrao, H., Dunbar, M.B., Singleton, A., Montagna, P., Barbola, P., Vogt, J.V., 2014. Magnitude of extreme heat waves in present climate and their projection in a warming world. J. Geophys. Res. 119, 12500–12512. http://dx.doi.org/10.1002/2014JD022098.

Sen, P., 1968. Estimates of the regression coefficient based on Kendall's Tau. J. Am. Stat. Assoc. 63, 1379–1389. http://dx.doi.org/10.1080/01621459.1968.10480934.

Silva, P., Bastos, A., Libonati, R., Rodrigues, J., DaCamara, C., 2019. Impacts of the 1.5 °C global warming target on future burned area in the Brazilian cerrado. For. Ecol. Manag. 446, 193–203. http://dx.doi.org/10.1016/j.foreco.2019.05.047.

Solman, S., Blzquez, J., 2019. Multiscale precipitation variability over south America: analysis of the added value of CORDEX RCM simulations. Clim. Dyn. 53, 1547–1565. http://dx.doi.org/10.1007/s00382-019-04689-1.

Solman, S., Sanchez, E., Samuelsson, P., Rocha, R., Li, L., Marengo, J., Pessacg, N., Remedio, A., Chou, S., Berbery, H., Le Treut, H., Castro, M., Jacob, D., 2013. Evaluation of an ensemble of regional climate model simulations over south America driven by the ERA-interim reanalysis: model performance and uncertainties. Clim. Dyn. 41, 1139–1157. http://dx.doi.org/10.1007/s00382-013-1667-2.

Sutanto, S., Vitolo, C., Di Napoli, C., D'Andrea, M., Van Lanen, H., 2020. Heatwaves, droughts, and fires: Exploring compound and cascading dry hazards at the pan-European scale. Environ. Int. 134, 105276. http://dx.doi.org/10.1016/j.envint.2019.105276.

Taschetto, A., Ambrizzi, T., 2012. Can Indian ocean SST anomalies influence south American rainfall? Clim. Dyn. 38, 1615–1628. http://dx.doi.org/10.1007/s00382-011-1165-3.

Teichmann, C., Jacob, D., Remedio, A.e.a., 2021. Assessing mean climate change signals in the global CORDEX-CORE ensemble. Clim. Dyn. 57, 1269–1292. http://dx.doi.org/10.1007/s00382-020-05494-x.

Theil, H., 1950. A rank-invariant method of linear and polynomial regression analysis. Indag. Math. 1, 467–482.

Thielen, D., Ramoni-Perazzi, P., Puche, M.L., Márquez, M., Quintero, J.I., Rojas, W., Soto-Werschitz, A., Thielen, K., Nunes, A., Libonati, R., 2021. The pantanal under siegeon the origin, dynamics and forecast of the megadrought severely affecting the largest wetland in the world. Water 13, 3034. http://dx.doi.org/10.3390/w13213034.

Tomas, W., Berlinck, C., Chiaravalloti, R.e.a., 2021. Distance sampling surveys reveal 17 million vertebrates directly killed by the 2020's wildfires in the pantanal, Brazil. Sci. Rep. 11, 23547. http://dx.doi.org/10.1038/s41598-021-02844-5.

Tomas, W.M., de Oliveira Roque, F., Morato, R.G., et al., 2019. Sustainability agenda for the pantanal wetland: Perspectives on a collaborative interface for science, policy, and decision-making. Trop. Conserv. Sci. http://dx.doi.org/10.1177/1940082919872634.

UNESCO, 2021. UNESCO world heritage centre - world heritage list. URL: https://whc.unesco.org/en/list/, last accessed: 12-01-2021.

van Vuuren, D., Stehfest, E., Elzen, M., Kram, T., Vliet, J., Deetman, S., Isaac, M., Goldewijk, K., Hof, A., Beltran, A., Oostenrijk, R., Ruijven, B., 2011. RCP2.6: exploring the possibility to keep global mean temperature increase below 2 °C. Clim. Change 109, 95. http://dx.doi.org/10.1007/s10584-011-0152-3.

Viganó, H.G., Souza, C., Neto, J., Cristaldo, M., Jesus, L., 2018. Prediction and modeling of forest fires in the pantanal. Rev. Bras. Meteorol. 33, 306–316. http://dx.doi.org/10.1590/0102-7786332012.

Wilks, D., 2011. Statistical Methods in the Atmospheric Sciences, Vol. 100. Academic Press.

Williams, A., Abatzoglou, J., 2016. Recent advances and remaining uncertainties in resolving past and future climate effects on global fire activity. Curr. Clim. Change Rep. 2, 14. http://dx.doi.org/10.1007/s40641-016-0031-0.